Supporting Information

The Role of Reversibility in the Enantioselective Conjugate Addition of α,α-Disubstituted Aldehydes to Nitro-Olefins Catalyzed by Primary Amine Thioureas

Yining Ji, Donna G. Blackmond*
Department of Chemistry, The Scripps Research Institute, La Jolla, CA 92037, US

blackmond@scripps.edu

Table of Contents:

1. Materials and General Procedures

Dichloromethane was dried using a Solvent Purification System (SPS). Methylene chloride-d2 was purchased from Cambridge Isotope Laboratories, Inc. (D, 99.9%) in bottles of 10 g. 2-Phenylpropanal (95%) and *trans*-β-nitrostyrene (98%) were purchased from Alfa Aesar and 2-phenylpropanal was always carefully distilled prior to use. (*R*)-2-Phenylpropanol and (*S*)-2-phenylpropanol were purchased from Sigma-Aldrich. 1-Nitro-prop-1-ene[1], the primary amine thiourea catalysts **4** [2] and **5**[2], (*R*)-2-phenylpropanal [3] and (*S*)-2-phenylpropanal[3] were synthesized following the method described in the literature.

NMR spectra were recorded on Bruker DRX-600 equipped with a 5 mm DCH cryoprobe, DRX-500, and AMX-400 instruments and calibrated using residual undeuterated solvent as an internal reference. The following abbreviations (or combinations thereof) were used to explain the multiplicities: s = singlet, d = doublet, t = triplet, m = multiplet, br =broad.

For compound **1**, high-performance liquid chromatography (HPLC) was performed on Hitachi L-7400 UV detector (λ = 300 nm) using Chiralcel-ODH column (0.46 x 25 cm) using hexane:^{i}PrOH 99:1 (10 μL/min). The retention times for the two enantiomers were: t_R (*R*) = 4.71 min, t_R (*S*) = 5.32 min.

For compound **3a**, high-performance liquid chromatography (HPLC) was performed on Hitachi L-7400 UV detector (λ = 254 nm) using Chiralcel-IA column (0.46 x 25 cm) using hexane:^{i}PrOH 95:5 (10 μL/min). The retention times for the different stereoisomers were: t_R (2*R*, 3*S*) = 7.13 min, t_R (2*S*, 3*R*) = 7.99 min, t_R (2*R*, 3*R*) = 6.89 min, t_R (2*S*, 3*S*) = 7.93 min.

For compound **3b**, high-performance liquid chromatography (HPLC) was performed on Hitachi L-7400 UV detectors (λ = 221 nm) using Daicel Chiralpack AS-H column using hexane:^{i}PrOH 95:5 (1 mL/min). The retention times for the two enantioners of the *syn*-**3b** isomer were: t_R (2*S*, 3*S*) = 15.98 min, t_R (2*R*, 3*R*) = 16.91 min.

[1] Melton, J.; McMurry, J. E. *J. Org. Chem.* **1975**, *40* (14), 2138-2139.
[2] Lalonde, M. P.; Chen, Y. G.; Jacobsen, E. N. *Angew. Chem. Int. Edit* **2006,** *45* (38), 6366-6370.
[3] Vogt, H.; Ceylan, S.; Kirschning, A. *Tetrahedron* **2010**, *66* (33), 6450-6456.

2. Calibration Curve for NMR Kinetics

All the experiments were performed in a Bruker DRX-500 instrument. A capillary with pyrazine was used as a reference (pyrazine δ_H = 8.56 ppm) to quantify the concentrations of the species. In order to obtain quantitative data, we measured the 90 degree flip angle (P1/4) and the longitudinal relaxation time (T1) for every species. All the species (**2a**/**2b** and **3a**/**3b**) minus 2-phenylpropanal **1** had relaxation times lower than 7 s (relaxation time for the pyrazine in dichloromethane). Therefore, in future kinetic studies, to assure that all signal integrations are quantitative, a relaxation delay (D1) of 50 s should be used.

To calibrate the capillary, we used six solutions of a known concentration of nitroolefins.

Nitrostryrene **2a**:

[**2a**] (M)	$\frac{integration\ of\ \mathbf{2a}}{integration\ of\ pyrazine} \cdot 100$
0.01	31.2
0.03	87.7
0.05	147.1
0.07	196.1
0.09	263.2
0.12	344.8

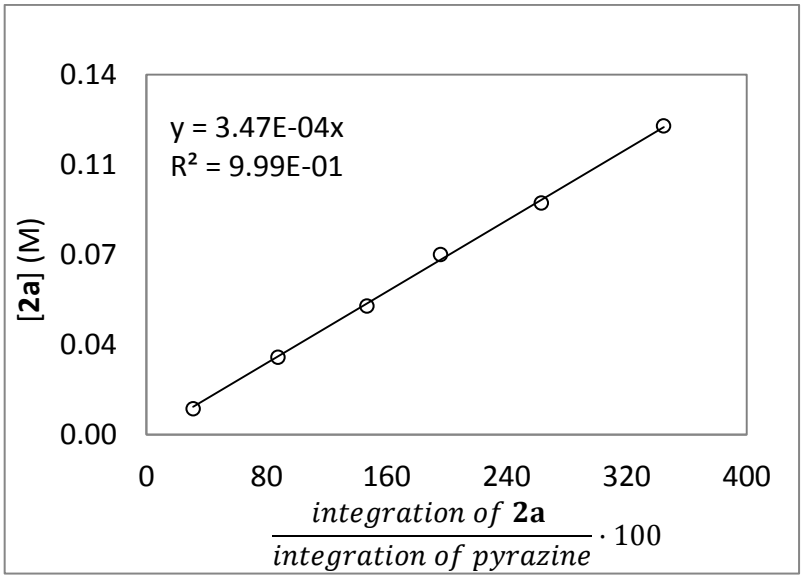

(*E*)-1-Nitro-1-propene **2b**:

[**2b**] (M)	$\frac{integration\ of\ \mathbf{2b}}{integration\ of\ pyrazine} \cdot 100$
0.05	144.9
0.07	212.8
0.09	263.2
0.11	322.6
0.13	384.6
0.15	454.5

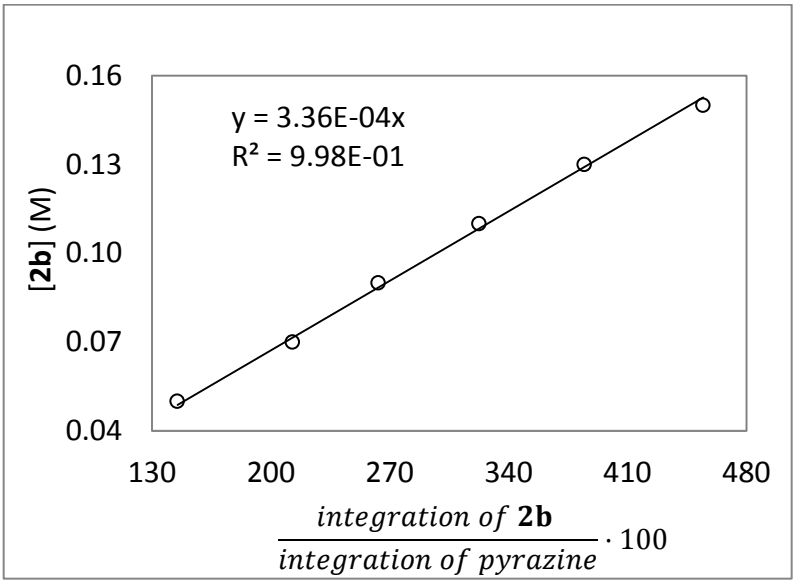

3. General Procedure for Kinetic Experiments:

0.4 mL (0.015 mmol) of a 0.0375 M solution of catalyst (**4** or **5**) in methylene chloride-d2 was placed in a NMR tube followed by addition of 50 μL of a fresh stock solution (3 M) of aldehyde. The reaction was initiated by the addition of 50 μL of a 1.5 M solution of nitro-olefins (**2a** or **2b**). Over reaction time, spectra of 4 scans with a 50 s acquisition delay (D1) between scans were registered. The spectra obtained were processed manually to obtain the concentration of each species during the reaction.

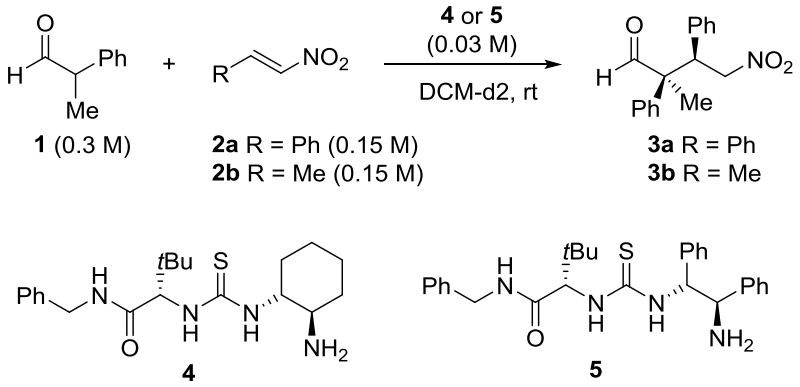

Scheme S1. Conjugate addition of α-phenylpropanal to nitro-olefins using primary amine thiourea catalysts.

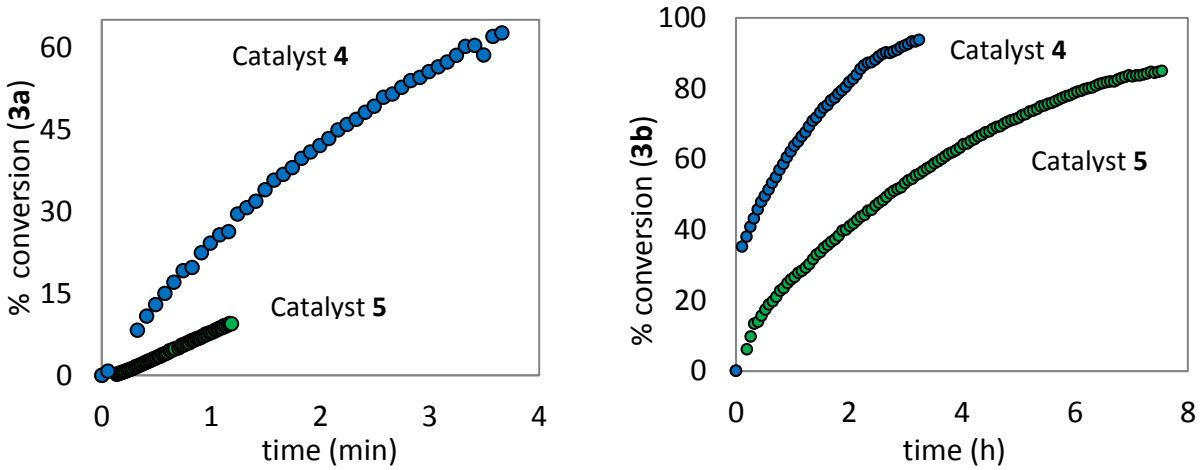

Figure S1. % conversion of product **3a** (left) and **3b** (right) as a function of time monitored by NMR spectroscopy for the reaction of Scheme S1 carried out using catalysts **4** and **5**.

3.1 Kinetic experiments (nitrostyrene **2a**)

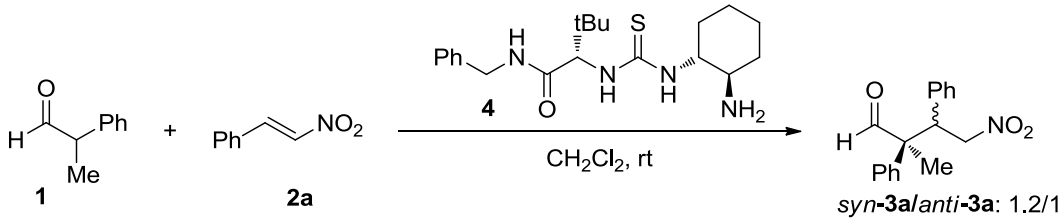

Scheme S2. Conjugate addition of α-phenylpropanal to nitrostyrene **2a** using catalyst **4**.

Table S1. Reaction conditions for kinetic experiments.

Reaction	$[\mathbf{1}]_0$ (M)	$[\mathbf{2a}]_0$ (M)	[excess] = $[\mathbf{2a}]_0$-$[\mathbf{1}]_0$ (M)
a	0.250	0.125	0.125 (same excess)
b	0.187	0.125	0.058 (different excess)
c	0.311	0.186	0.125 (same excess)

"Same" and "different" excess experiments:

Figure S2 plots the temporal concentration profiles for two "same excess" experiments **a** and **c** in Table S1 designed to test catalyst stability. The temporal concentrations of **1** and **2a** at the beginning of reaction **a** (blue circles) are identical to those that reaction **c** (red circles) reaches after ca. 3 h. Comparison of the profiles of these two reactions from a point of identical concentrations of the two substrates is made possible by shifting the curve from reaction **a** in time, as shown by the gray arrows in Figure S2 to give the adjusted curve shown in blue hollow circles. Two reactions under identical conditions should give identical temporal profiles. However, it is clear that reaction **a** proceeds somewhat faster than reaction **c** from this point onward. The fact that the "time adjusted" profile of reaction **a** does not overlay onto that of reaction **c** suggests that some process other than the intrinsic kinetics related to the temporal substrate concentrations [**1**] and [**2a**] contributes to the observed reaction rate. Likely candidates for processes that result in such behavior are irreversible catalyst deactivation or product inhibition (reversible catalyst deactivation).

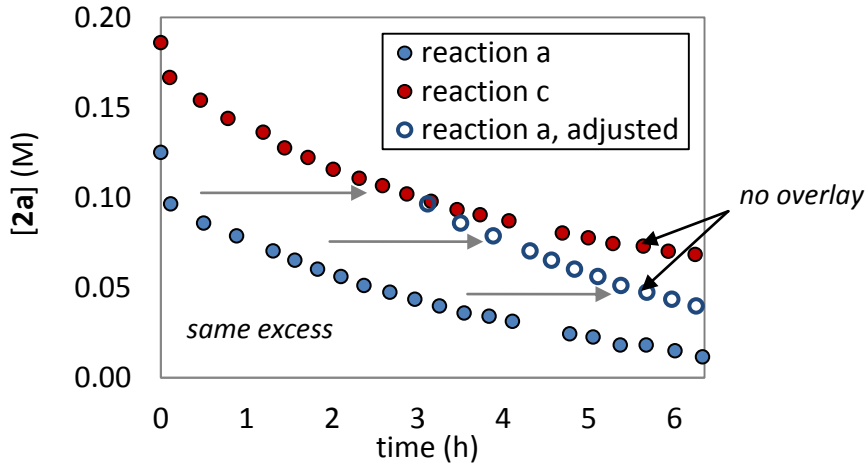

Figure S2. Temporal concentration profiles monitored by NMR spectroscopy for the reaction of Scheme S2 carried out under the "same excess" conditions noted in Table S1. The "adjusted" profile is shifted horizontally along the time x-axis as described in the text.

It is interesting to note that the initial slopes of the two reactions under conditions **a** and **c** in Figure S2 appear to be similar. This is confirmed by comparing these reaction profiles using another type of "adjusted" profile, as shown in Figure S3. A simple graphical manipulation moves the reaction **a** data (blue circles) vertically upward, as indicated by the gray arrows, to produce the profile given by the blue hollow circles. Identical slopes on plots of [**2a**] vs time confirm identical reaction rates for these two reactions, yet at any given point in time, these two reactions exhibit different concentrations of both reactants **1** and **2a**. Thus, Figure S3 indicates that the reaction must be zero order in [**1**] and zero order in [**2a**].

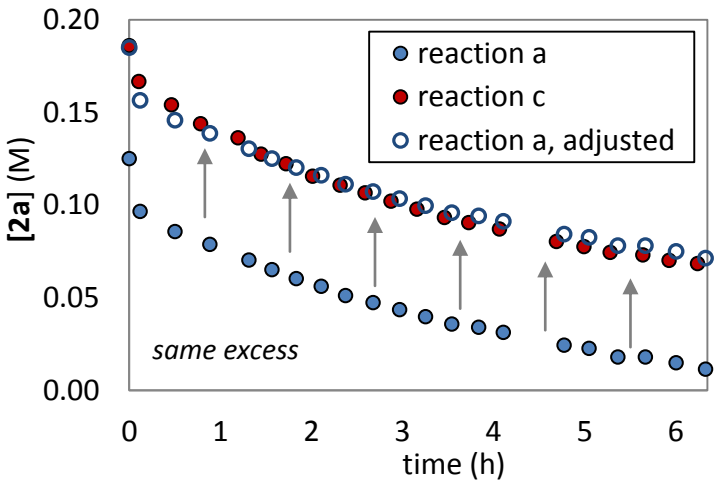

Figure S3. Temporal concentration profiles monitored by NMR spectroscopy for the reaction of Scheme S2 carried out under the "same excess" conditions noted in Table S1. The "adjusted" profile is shifted vertically along the concentration y-axis as described in the text.

The suggestion of zero order kinetics in [**1**] is confirmed by the concentration profiles in Figure S4 showing the results of the two "different excess" experiments, which are designed to probe the reaction order in substrates. The two curves from the two reactions carried out with identical initial $[\mathbf{2a}]_0$ but different $[\mathbf{1}]_0$ are found to overlay for at least to first 50% conversion. These identical slopes, indicating identical reaction rates, for two experiments carried out using different quantities of the aldehyde **1**, indicate that the reaction exhibits zero order kinetics in [**1**] at the beginning of the reaction.

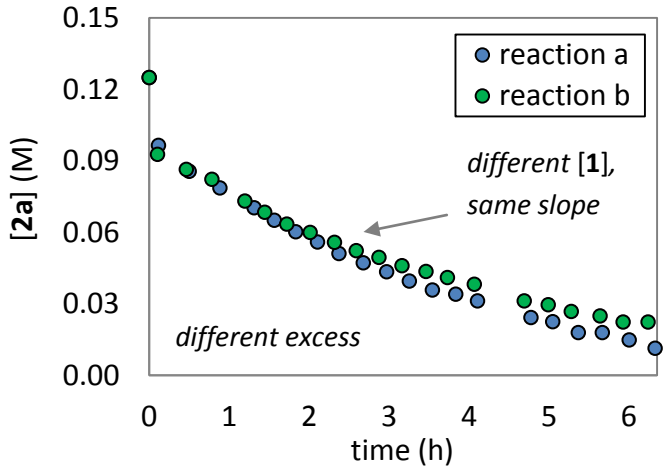

Figure S4. Temporal concentration profiles monitored by NMR spectroscopy for the reaction of Scheme S2 carried out under the "different excess" conditions noted in Table S1.

3.2 Kinetic experiments ((1*E*)-1-nitro-1-propene **2b**)

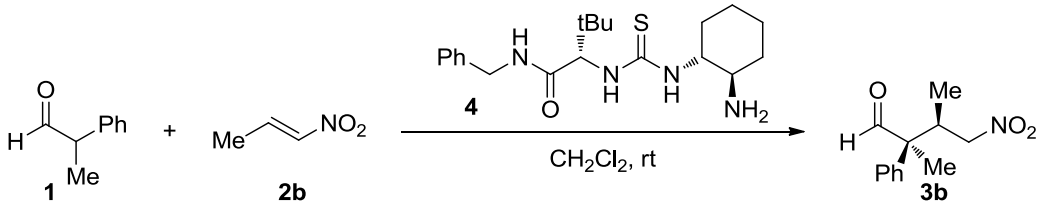

Scheme S3. Conjugate addition of α-phenylpropanal to (*E*)-1-nitro-1-propene **2b** using catalyst **4**.

Table S2. Reaction conditions for kinetic experiments.

Reaction	$[\mathbf{1}]_0$ (M)	$[\mathbf{2b}]_0$ (M)	[excess] = $[\mathbf{2b}]_0$-$[\mathbf{1}]_0$ (M)
a	0.150	0.300	0.150 (same excess)
b	0.150	0.224	0.074 (different excess)
c	0.233	0.373	0.150 (same excess)

"Same" and "different" excess experiments:

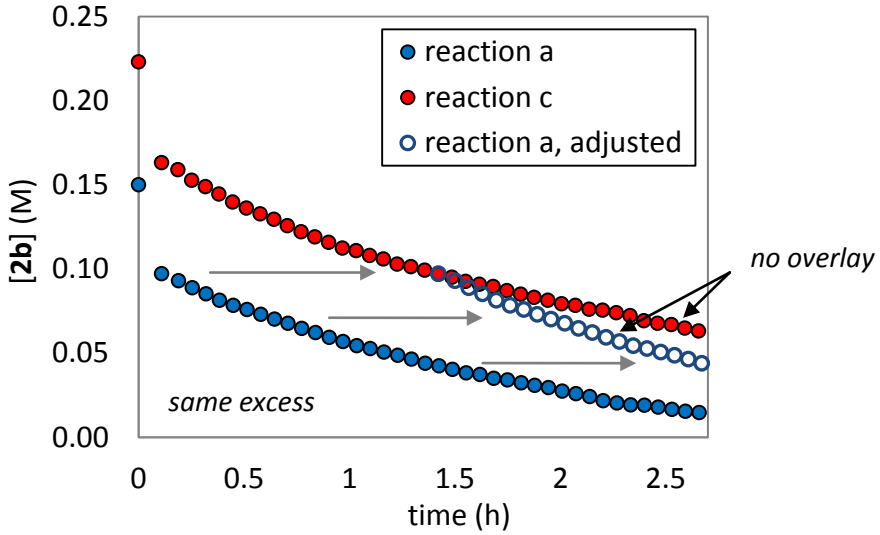

Figure S5. Temporal concentration profiles monitored by NMR spectroscopy for the reaction of Scheme S3 carried out under the "same excess" conditions noted in Table S2. The "adjusted" profile is shifted horizontally along the time x-axis. And similarly to **2a**, the fact that the "time adjusted" profile of reaction **a** (blue hollow circles) does not overlay onto that of reaction **c** (red circles) suggests either irreversible catalyst deactivation or product inhibition.

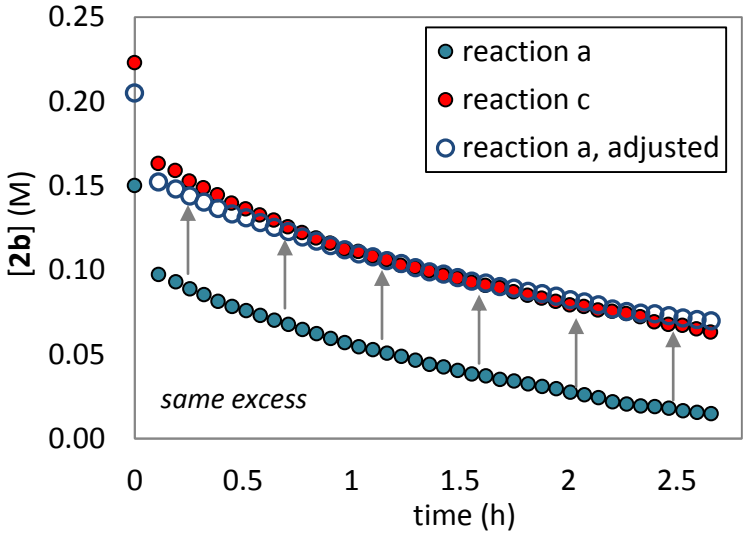

Figure S6. Temporal concentration profiles monitored by NMR spectroscopy for the reaction of Scheme S3 out under the "same excess" conditions noted in Table S2. The "adjusted" profile is shifted vertically along the concentration y-axis. And like **2b**, the identical slopes on plots of [**2b**] vs time (identical reaction rates for these two reactions, yet at any given point in time, these two reactions exhibit different concentrations of both reactants **1** and **2b**) confirms that the reaction must be zero order in [**1**] and zero order in [**2b**].

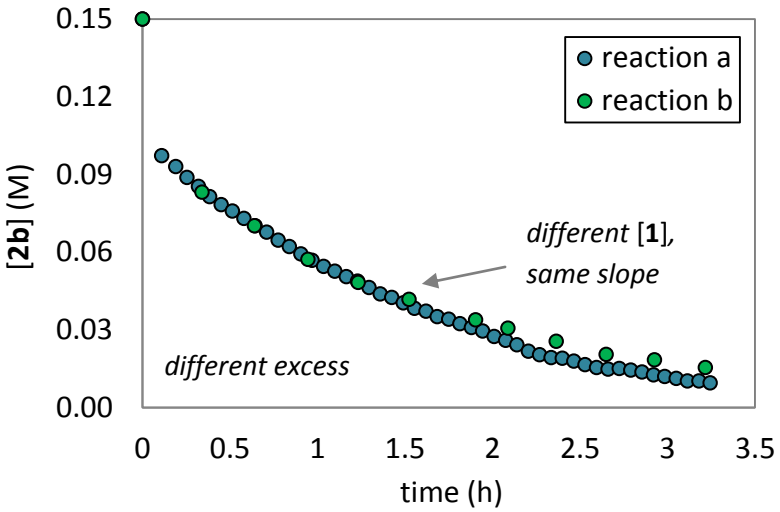

Figure S7. Temporal concentration profiles monitored by NMR spectroscopy for the reaction of Scheme S3 carried out under the "different excess" conditions noted in Table S2. The identical slopes at the beginning of the reaction for two experiments carried out using different quantities of the aldehyde **1**, indicate that the reaction exhibits zero order kinetics in [**1**].

4. Effect of the Chirality of 2-Phenylpropanal on the Enantio- and Diastereoselectivity

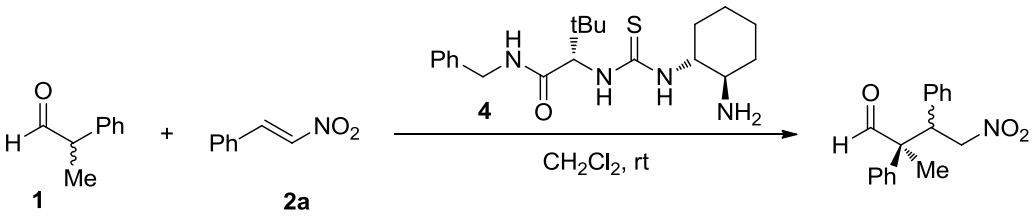

Table S3: Selectivity observed by using rac-**1**, (*R*)-**1** or (*S*)-**1** in the conjugate addition of α-phenylpropanal to nitrostyrene **2a** catalyzed by catalyst **4**.

	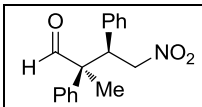 *syn*-**3a**	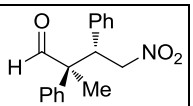 *anti*-**3a**
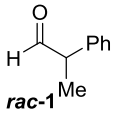 ***rac*-1**	1.2 (66% *ee*)	1 (3% *ee*)
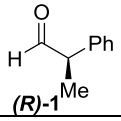 ***(R)*-1**	2.8 (87% *ee*)	1 (18% *ee*)
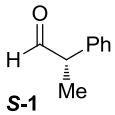 ***S*-1**	2.3 (85% *ee*)	1 (3% *ee*)

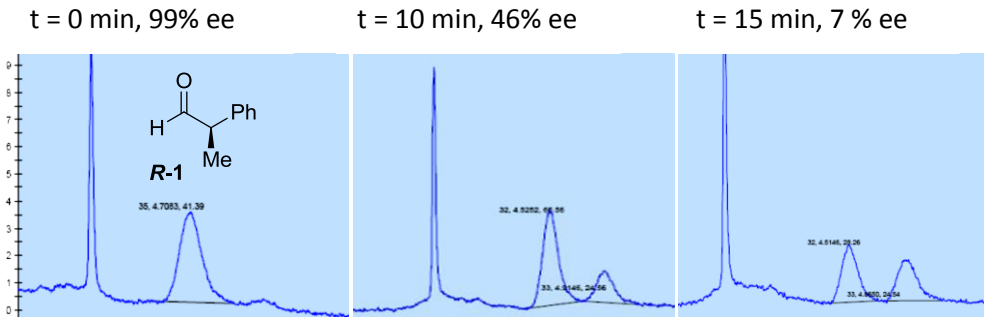

Figure S8: HPLC chromatograms showing the fast racemization of (*R*)-**1** in the reaction mixture over time.

5. General Procedure for Kinetic Experiments of the Backward Reaction

0.4 mL of a freshly prepared stock solution of catalyst (0.015 mmol) in methylene chloride-d2 was placed in an NMR tube containing the *syn* or *anti* product (0.075 mmol). The solution was shakn by hand and this time was taken as time zero. Over reaction time, spectra of 4 scans with a 50 s acquisition delay (**D1**) between scans were registered. The spectra obtained were processed manually to obtain the concentration of each species during the reaction.

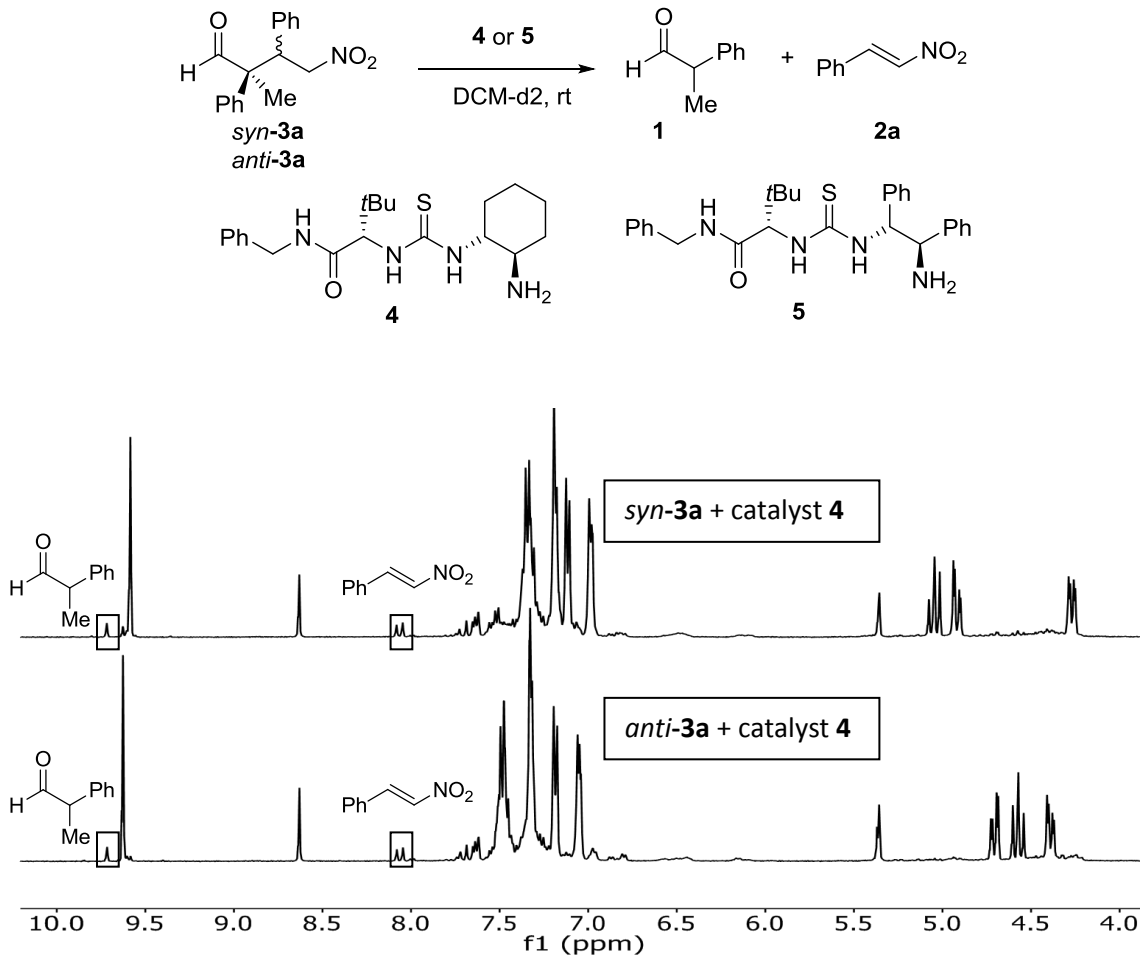

Figure S9: NMR spectra showing the presence of nitrostyrene **2a** and α-propionaldehyde **1** at 12h upon interaction of *syn*-**3a** and *anti*-**3a** with thiourea catalyst **4**.

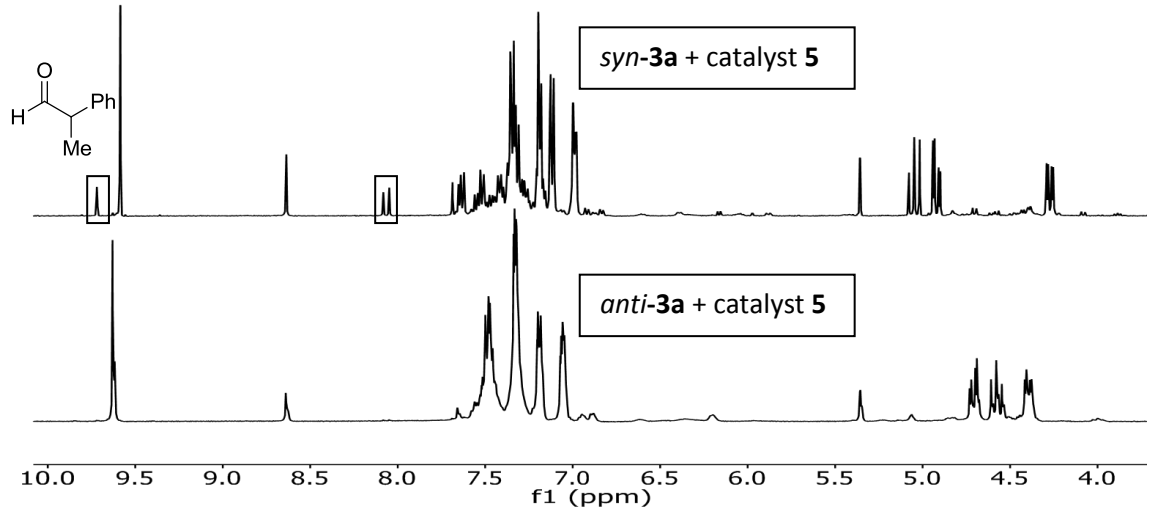

Figure S10: NMR spectra showing respectively the presence and absence of nitrostyrene **2a** and α-propionaldehyde **1** at 12h upon the interaction of *syn*-**3a** and *anti*-**3a** with catalyst **5**.

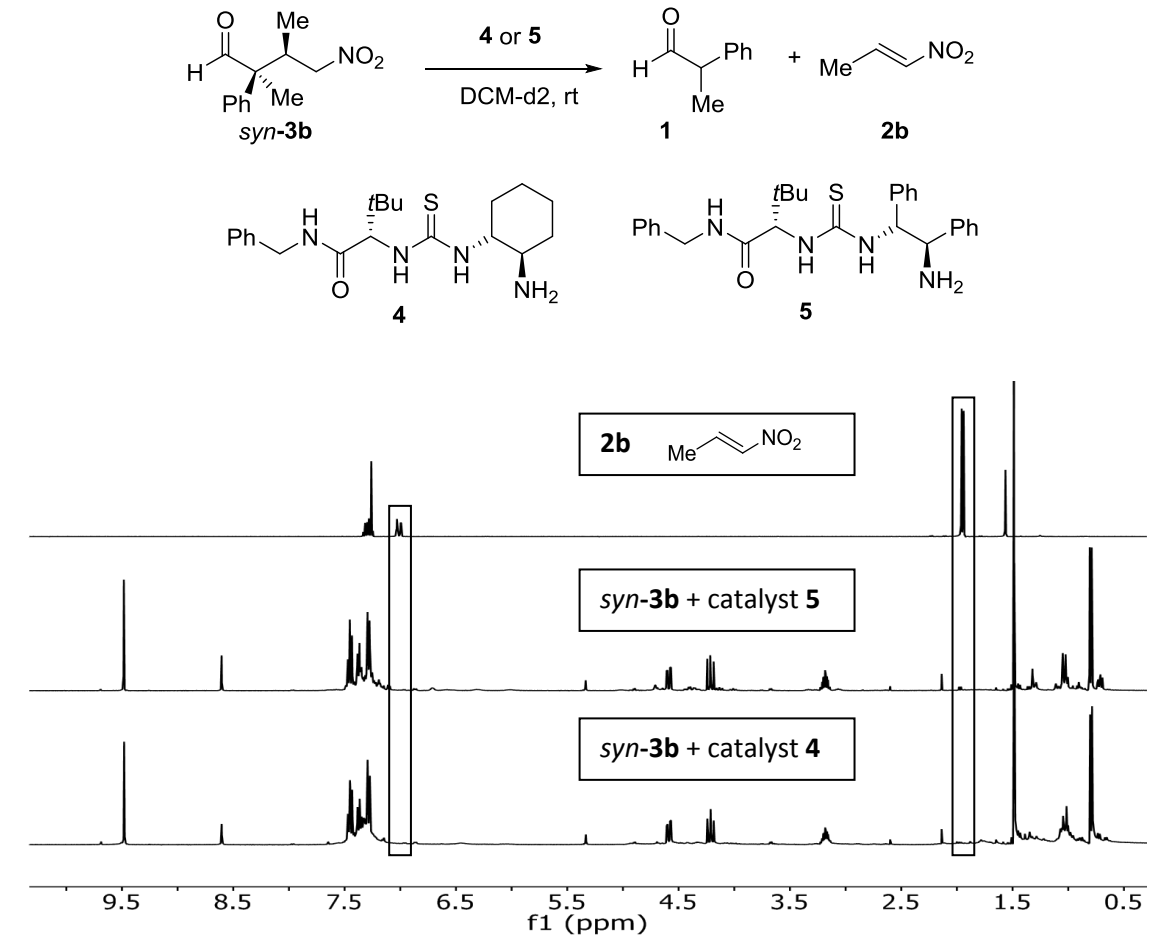

Figure S11: NMR spectra showing the absence of (*E*)-1-nitro-1-propene **2b** and α-propionaldehyde **1** at 12h upon interaction of *syn*-**3b** with catalysts **4** and **5**.

6. Reaction Intermediates

*6.1 Identification of imine **6**:*

A 0.025 M solution of the thiourea catalyst **4** (0.015 mmol) in methylene chloride-d2 was placed in a NMR tube in presence of 4Å molecular sieves. Freshly distilled 2-phenylpropanal (2 μL, 0.015 mmol) was added to form imine **6**.

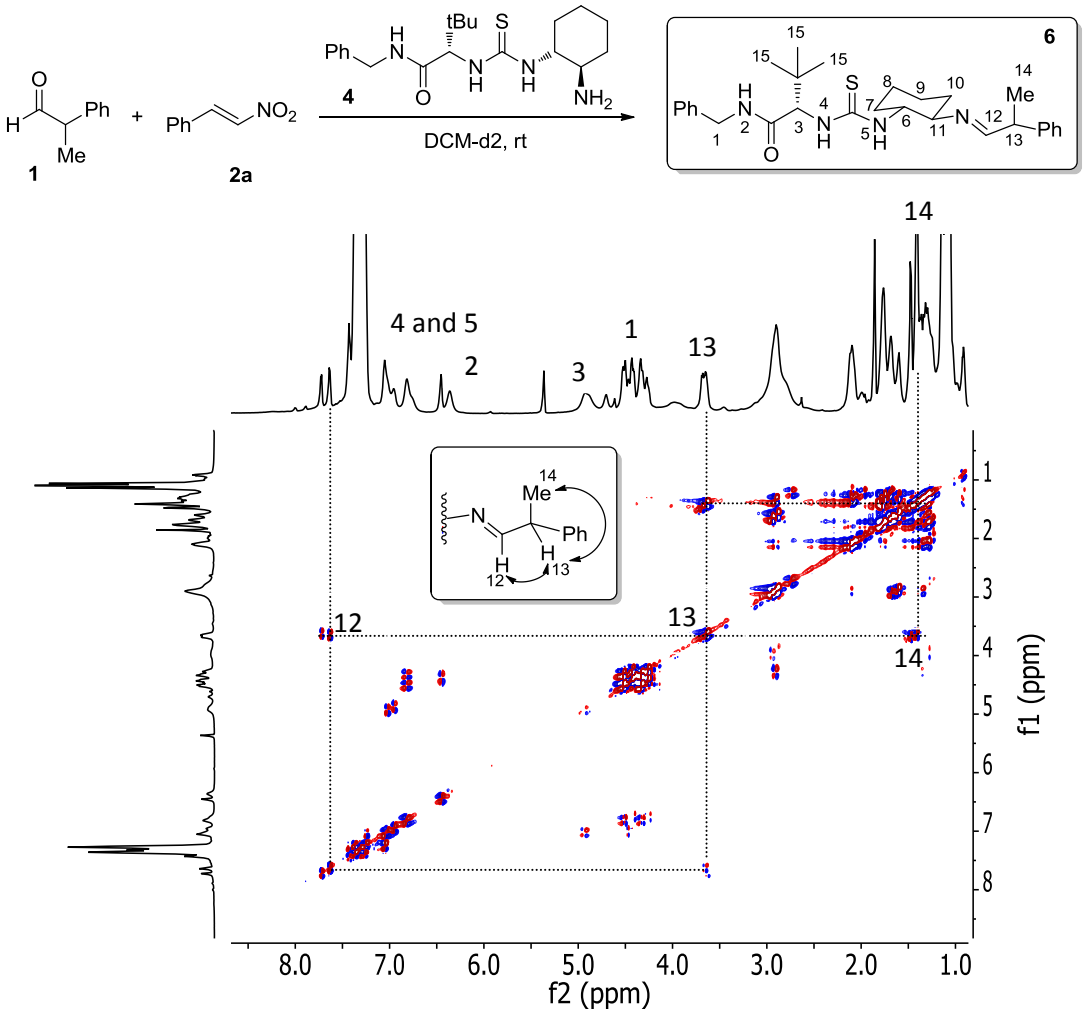

Figure S12. COSY of imine **6**. The cross peaks between H12-H13 and H13-H14 confirm the formation of the imine **6** instead of the corresponding enamine **7**, in which no proton is present in position 13.

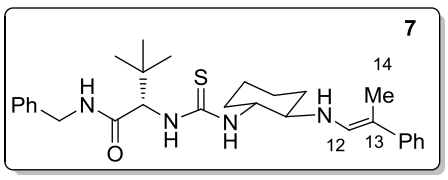

*6.2a Identification of product imines (syn-**8a** and anti-**8b**):*

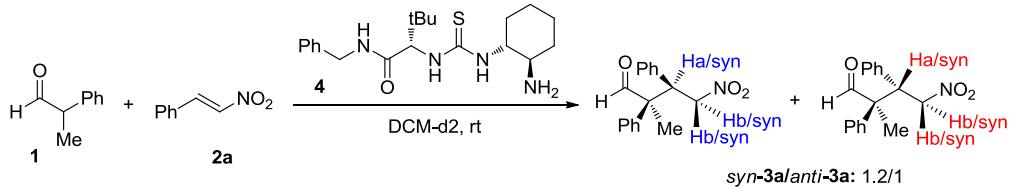

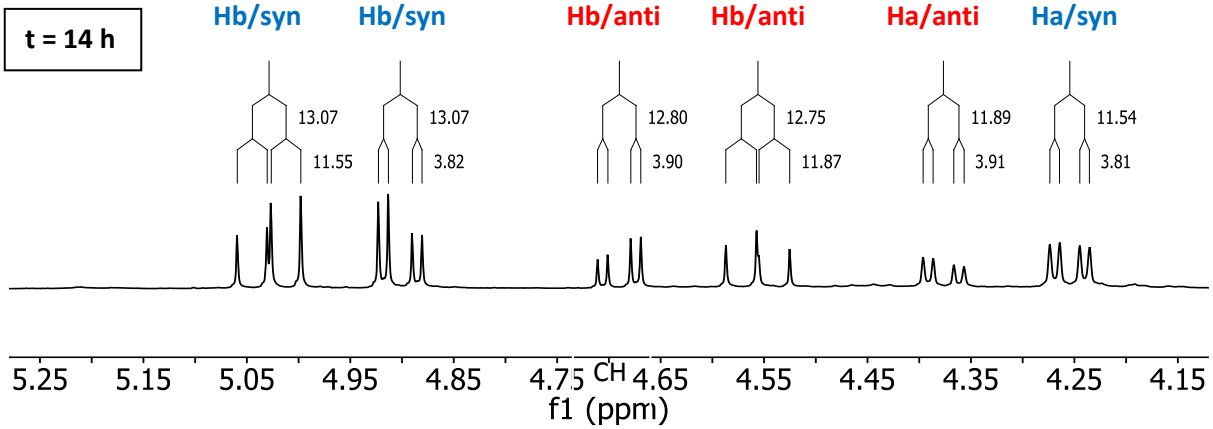

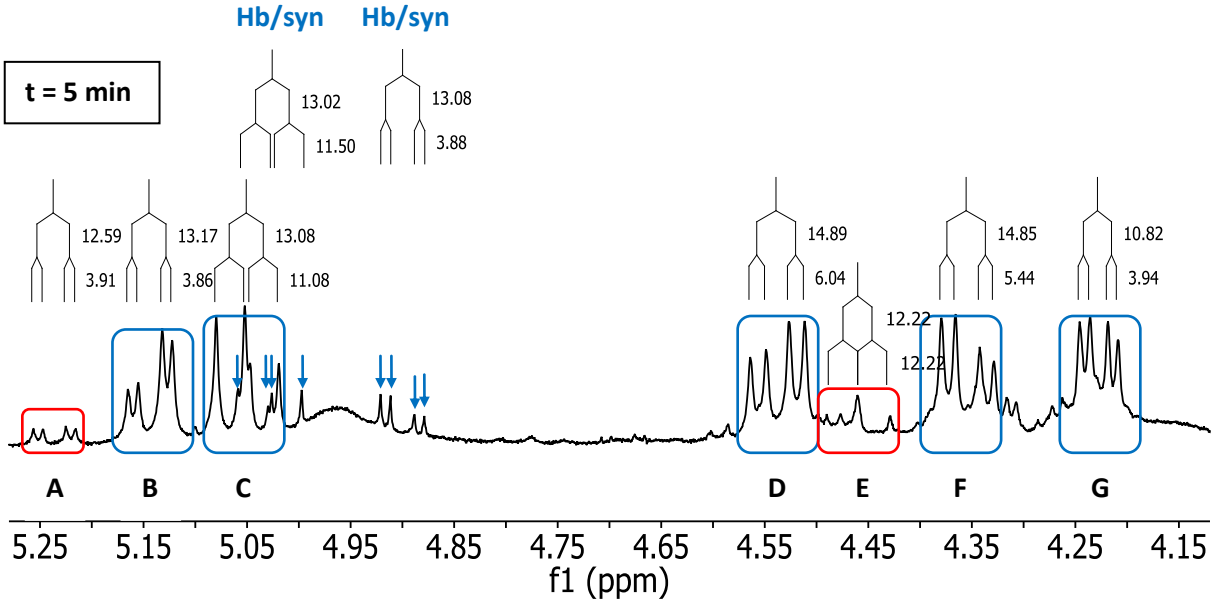

Figure S13: NMR spectra of the reaction recorded at t = 5 min and t = 14 h. For the spectrum at t = 5 min, the signals indicated by blue arrows correspond to *syn*-**3a** and all the signals marked in squares (A-G) are transient reaction intermediates. One minor (red square, A and E) and one major (blue square, B, C and G) intermediate species can be identified. The minor intermediate would give rise to the *anti* isomer because both the signal A (dd, *J* = 12.6 and 3.9 Hz) and E (dd, *J* = 12.2 and 12.2 Hz) display nearly identical coupling constants to those from *anti*-**3a** (dd, *J* = 12.8 and 3.9 Hz and dd, *J* = 12.7 and 11.9 Hz). Furthermore, the major isomer would provide the *syn* isomer since B (dd, *J* = 13.2 and 3.9 Hz), C (dd, *J* = 13.1 and 11.1 Hz) and G (dd, *J* = 10.8 and 3.9 Hz) exhibit coupling constants very close to the signals corresponding to *syn*-**3a** (dd, *J* = 13.1 and 3.9 Hz, dd, *J* = 13.1 and 11.5 Hz and dd, *J* = 11.5 and 3.8 Hz).

*6.2b Characterization of product imines (syn-**8a**, syn-**8b**, syn-**9a** and syn-**9b**):*

A 0.025 M solution of the thiourea catalysts **4** or **5** (0.015 mmol) in methylene chloride-d2 was placed in a NMR tube in the presence of 4Å molecular sieves. Freshly distilled 2-phenylpropanal (2 μL, 0.015 mmol) was added and the NMR tube was then equilibrated to 0 ^{o}C. The product imines can be provided quantitatively by the addition of 50 μL of a stock solution of the corresponding nitro-olefin (0.015 mmol).

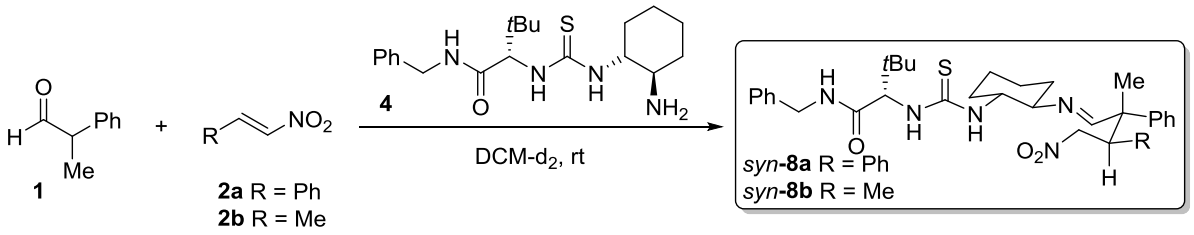

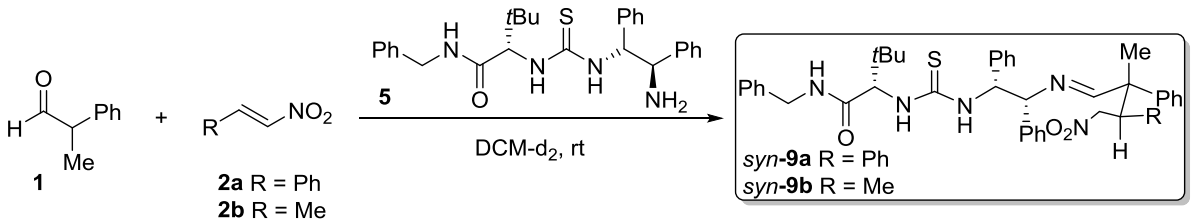

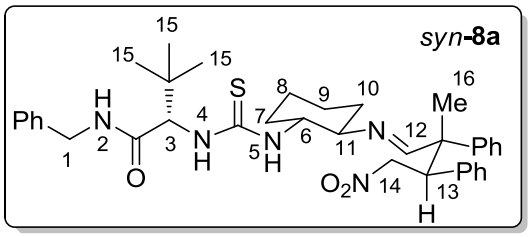

^{1}H NMR (400 MHz, $CDCl_3$) δ 1.07 (s, 9H, CH_3), 1.20-1.36 (m, 1H, CH_2; 2H, CH_2), 1.40 (s, 3H, CH_3), 1.70 (br s, 2H, CH_2), 1.78 (br s, 2H, CH_2), 2.16 (br s, 2H, CH_2), 3.02 (br s 1H, CH), 4.19 (dd, J = 11 and 4 Hz, 1H, CH), 4.25-4.34 (m, 1H, CH_2), 4.50 (dd, J = 15 and 6 Hz, 1H, CH_2), 4.99 (t, J = 12 Hz, 1H, CH_2), 5.08-5.17 (m, 1H, CH_2), 6.12 (br s, 1H, NH), 6.45 (br s, 2H, NH) ppm; ^{13}C NMR (100 MHz, $CDCl_3$) δ 18.9 (CH_3), 24.0 (CH_2), 24.7 (CH_2), 27.1 ($3CH_3$), 31.9 (CH_2), 33.7 (CH_2), 43.8 (CH_2), 50.0 (C), 51.2 (CH), 77.2 (CH_2), 167.4 (CH) ppm.

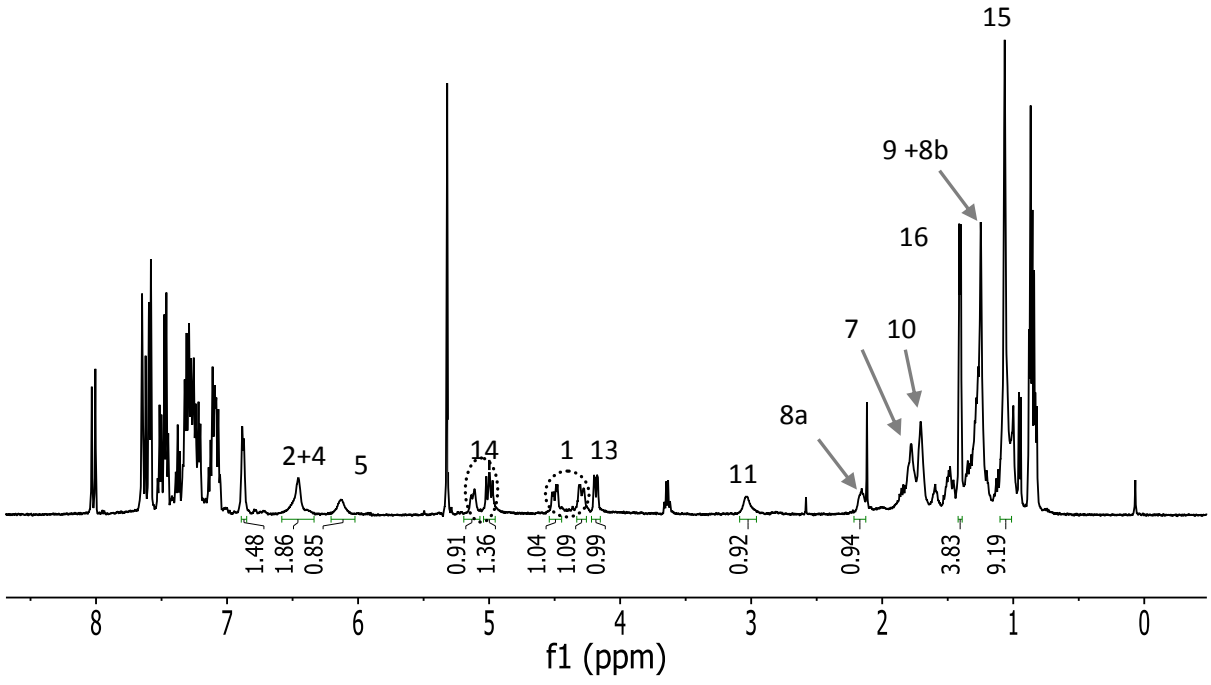

Figure S14. ^{1}H-NMR of *syn*-**8a**.

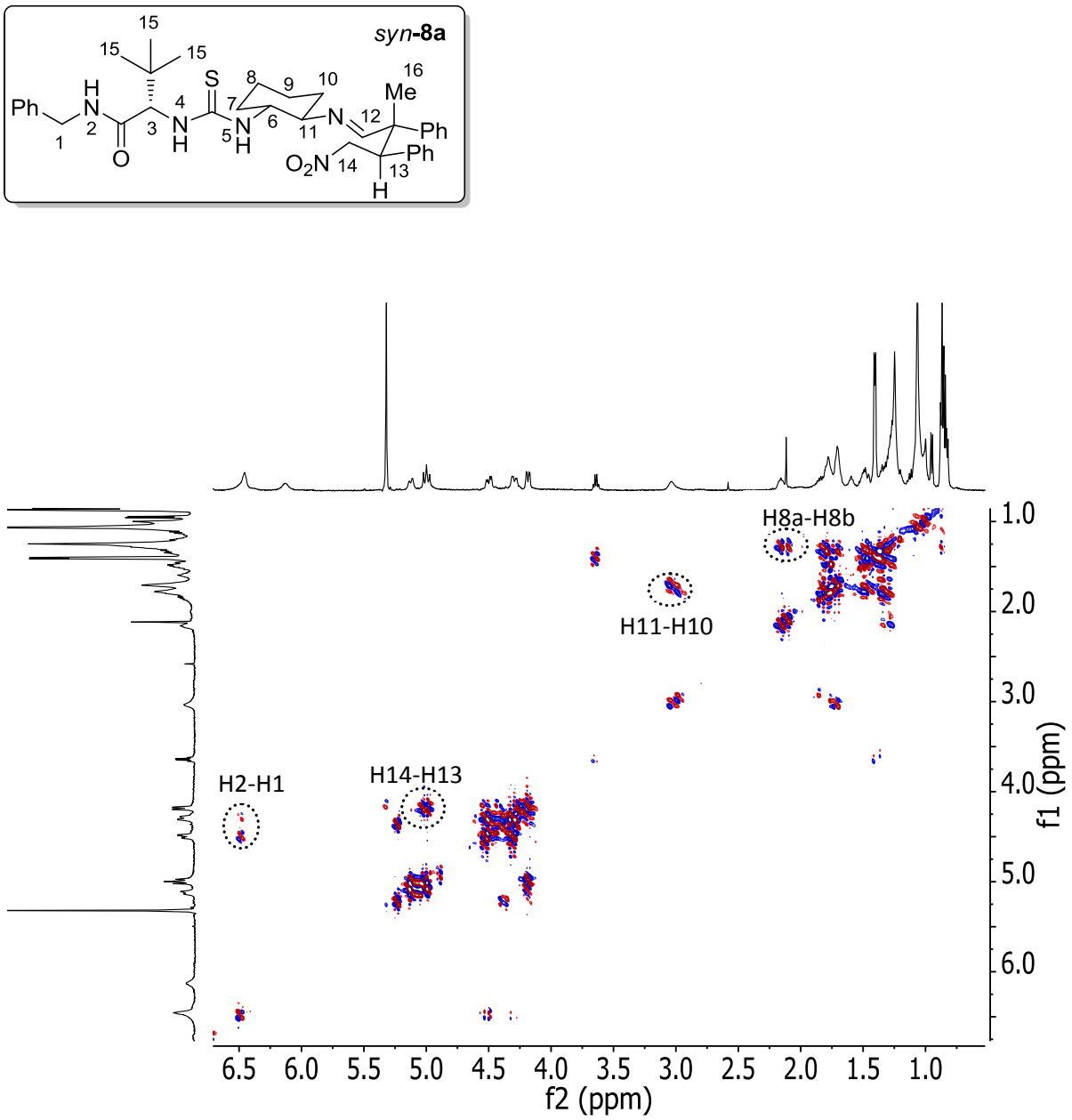

Figure S15. COSY of *syn*-**8a**.

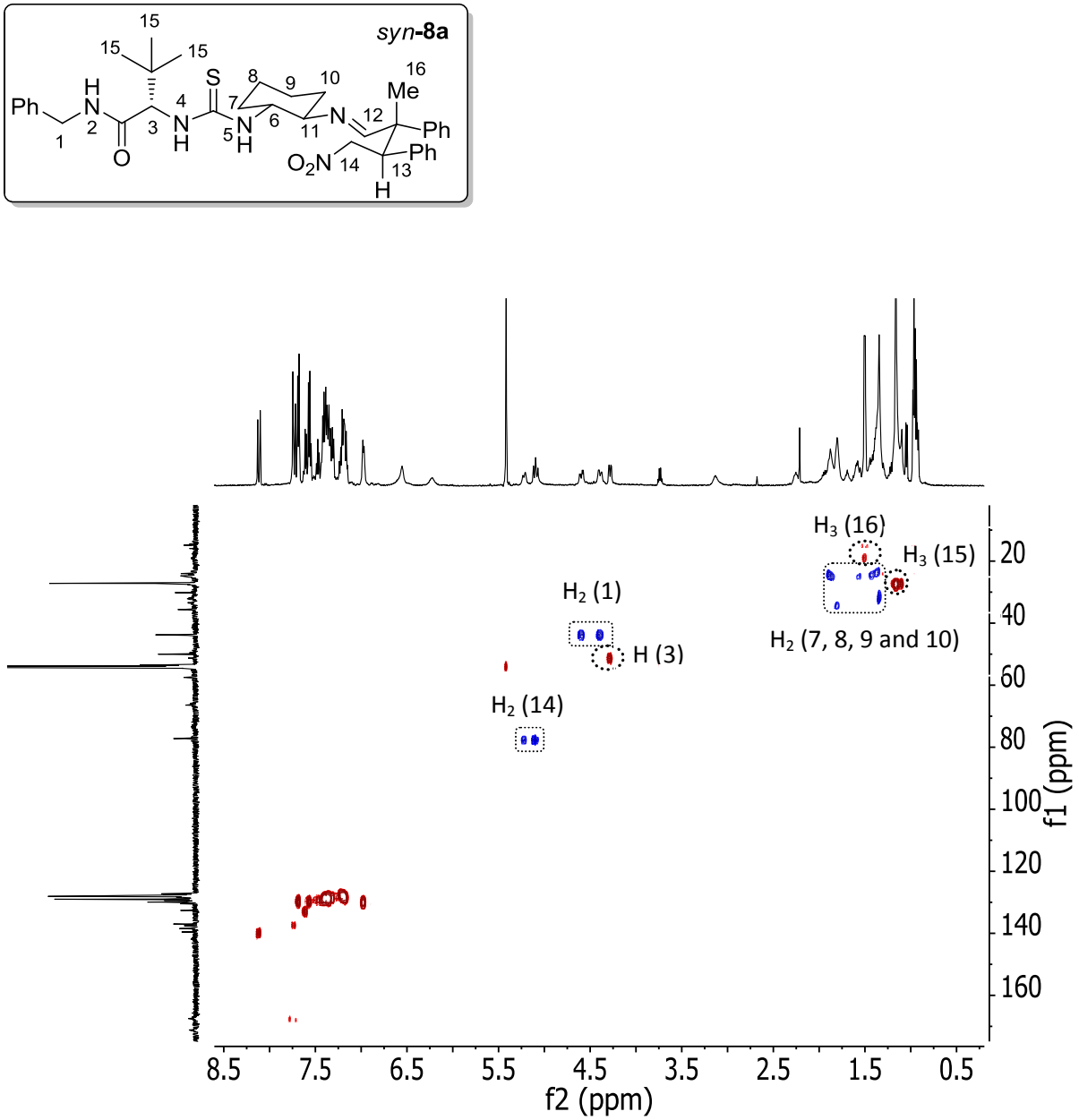

Figure S16. HSQC of *syn*-**8a**.

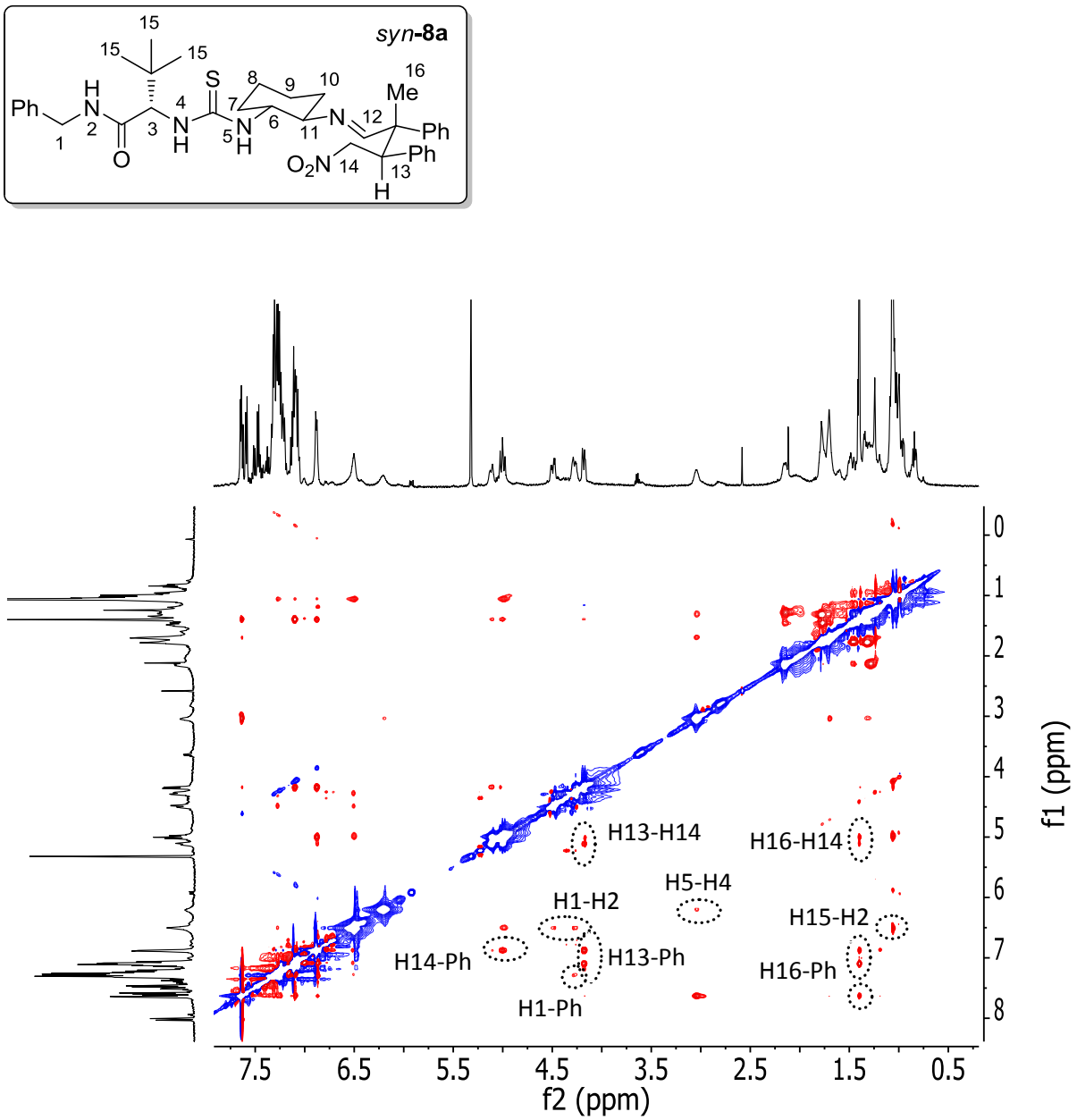

Figure S17. NOESY of *syn*-**8a**.

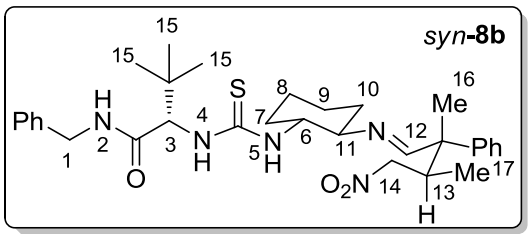

^{1}H NMR (400 MHz, $CDCl_3$) δ 0.72 (d, J = 7 Hz, 3H, CH_3), 1.01 (s, 9H, CH_3), 1.16-1.31 (m, 1H, CH_2; 2H, CH_2), 1.35 (s, 3H, CH_3), 1.37-1.47 (m, 1H, CH_2), 1.60 (br s, 2H, CH_2), 1.72 (br s, 2H, CH_2), 2.11 (br s, 2H, CH_2), 2.94 (br s 1H, CH), 3.05 (br s, 1H, CH), 4.18 (t, J = 11 Hz, 1H, CH_2), 4.23-4.33 (m, 1H, CH_2), 4.41-4.51 (m, 1H, CH_2), 4.61-4.71 (m, 1H, CH_2), 4.88 (br s, 1H, CH), 6.05 (br s, 1H, NH), 6.05 (br s, 2H, NH), 7.19-7.34 (m, 8H, CH), 7.34-7.43 (m, 2H, CH), 7.60 (br s, 1H, CH) ppm; ^{13}C NMR (100 MHz, $CDCl_3$) δ 13.3 (CH_3), 17.9 (CH_3), 24.0 (CH_2), 24.8 (CH_2), 27.0 ($3CH_3$), 31.8 (CH_2), 33.7 (CH_2), 35.3 (C), 39.3 (CH), 43.8 (CH_2), 49.3 (C), 66.3 (CH), 73.2 (CH), 79.8 (CH_2), 128.1 (CH), 129.0 (CH), 138.5 (C), 167.5 (CH) ppm.

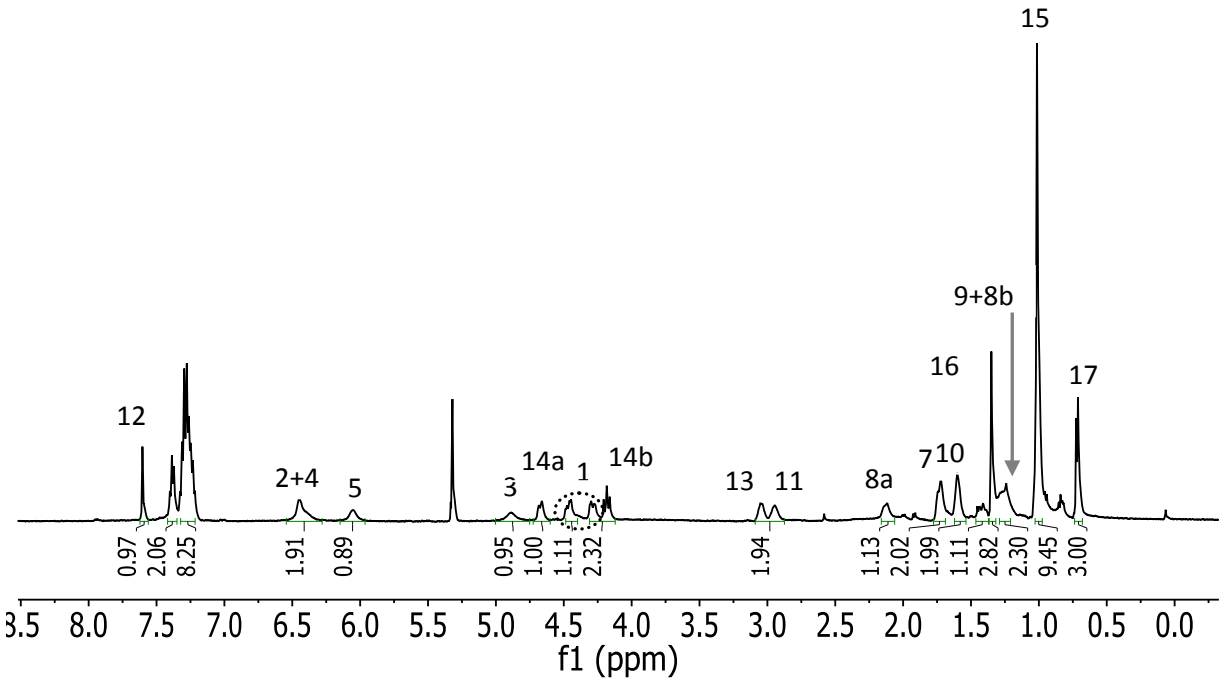

Figure S18. ^{1}H-NMR of *syn*-**8b**.

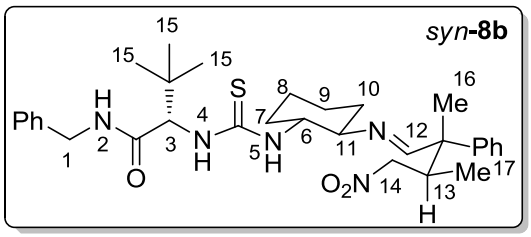

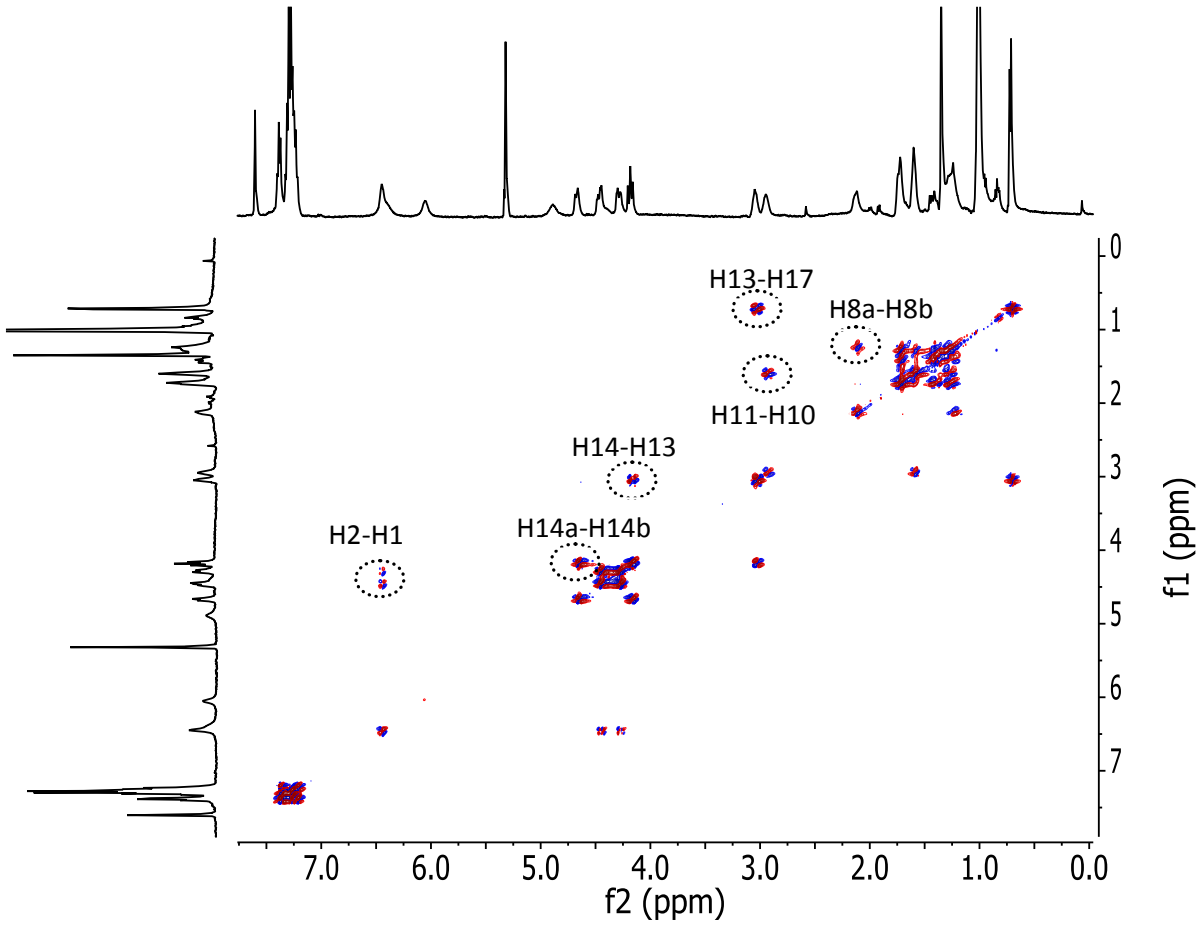

Figure S19. COSY of *syn*-**8b**.

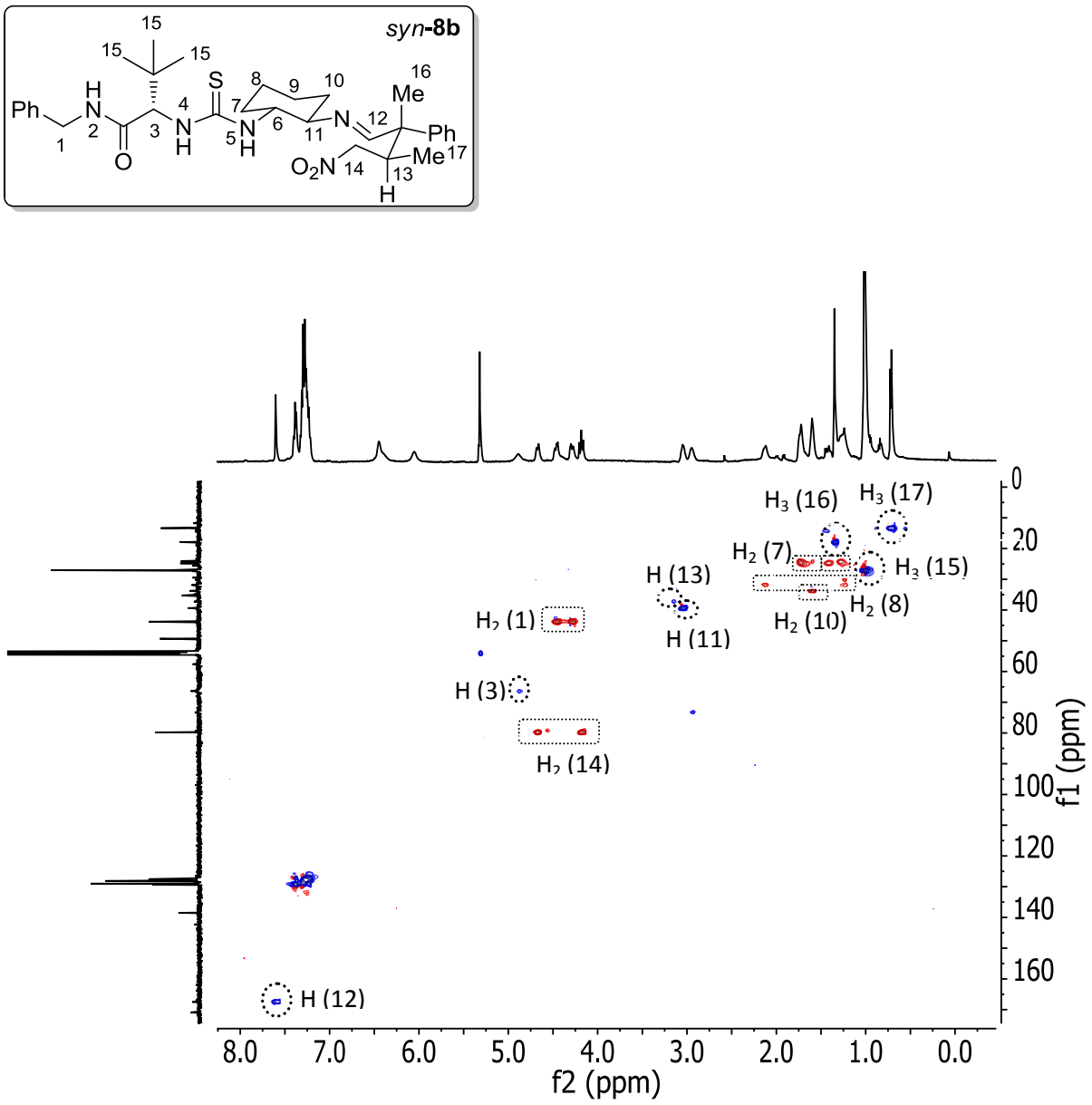

Figure S20. HSQC of *syn*-**8b**.

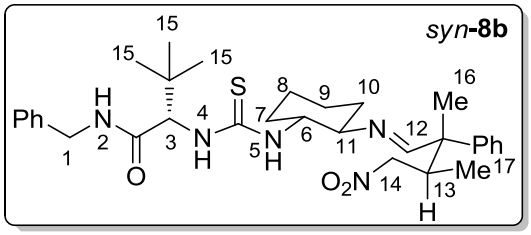

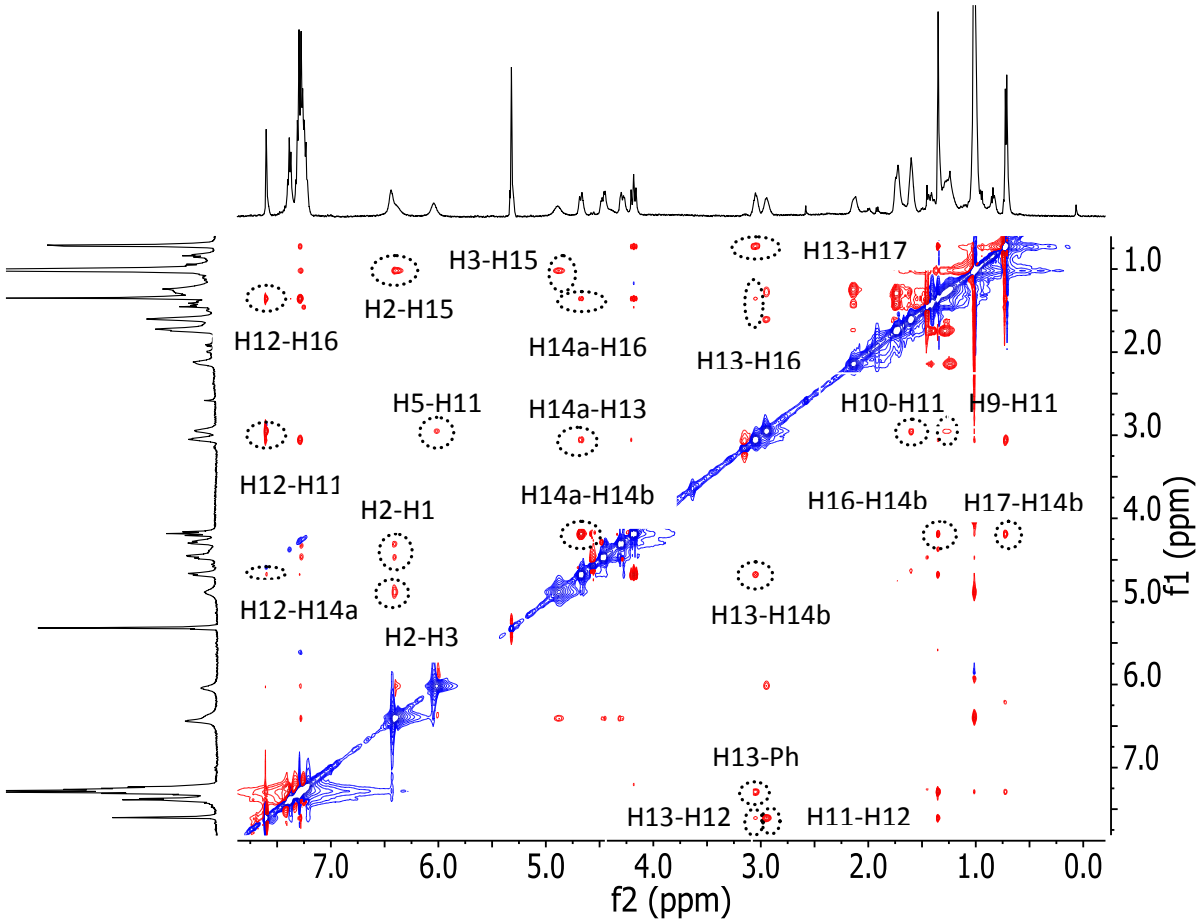

Figure S21. NOESY of *syn*-**8b**.

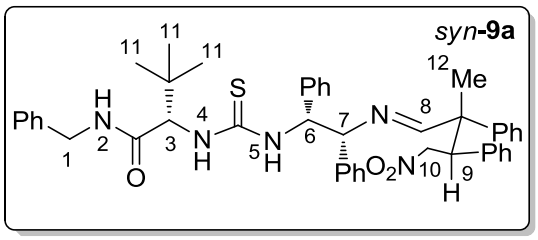

^{1}H NMR (400 MHz, $CDCl_3$) δ 1.01 (s, 9H, CH_3), 1.45 (s, 3H, CH_3), 4.17 (d, J = 10 Hz, 1H, CH), 4.26-4.35 (m, 1H, CH_2), 4.35-4.43 (m, 1H, CH_2), 4.77 (br s, 1H, CH), 4.89 (t, J = 11 Hz, 1H, CH_2), 5.43 (br s, 1H, CH_2) ppm; ^{13}C NMR (100 MHz, $CDCl_3$) δ 16.6 (CH_3), 26.9 (CH_3), 43.6 (CH_2), 52.0 (CH), 77.9 (CH), 79.0 (CH_2), 171.7 (CH) ppm.

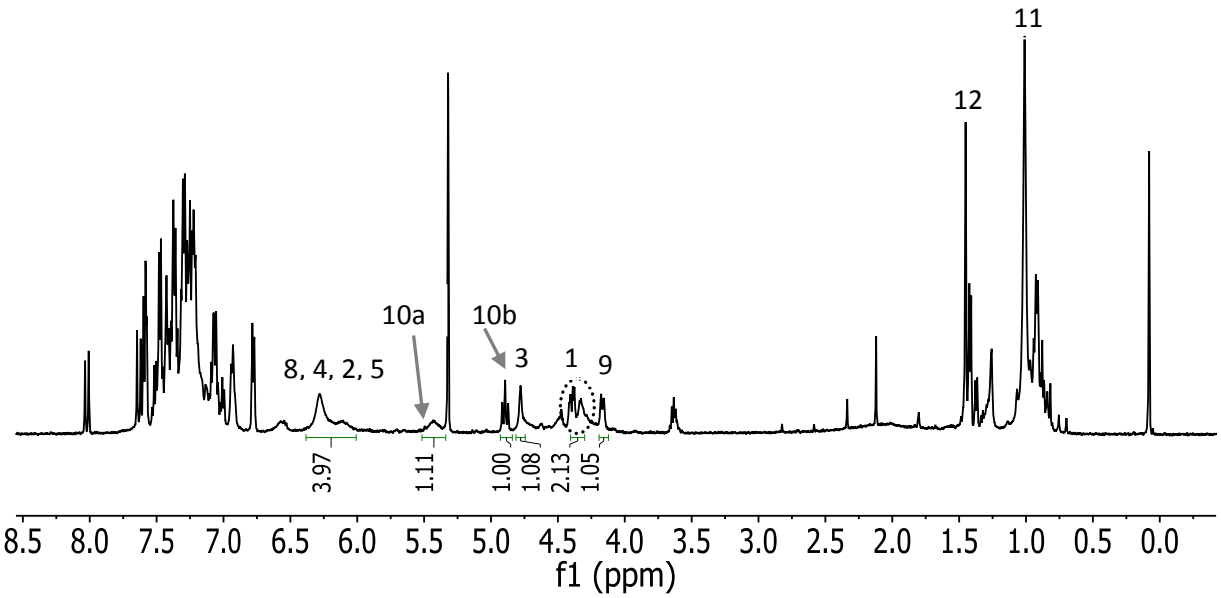

Figure S22. ^{1}H-NMR of *syn*-**9a**.

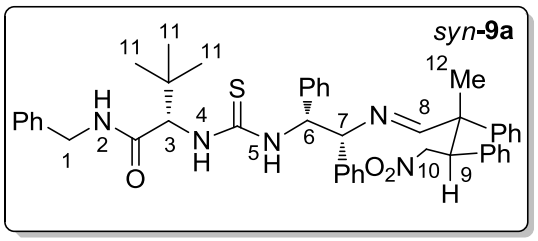

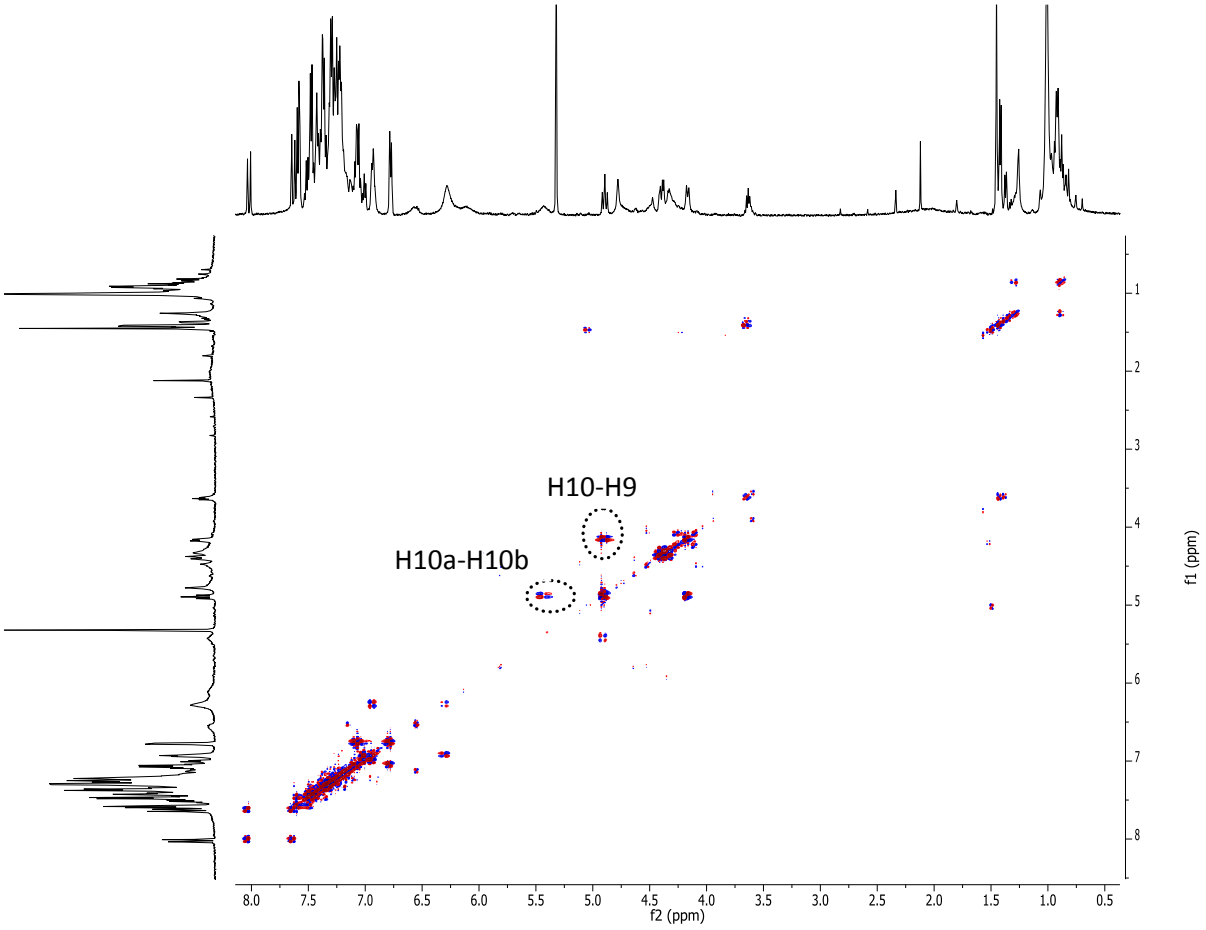

Figure S23. COSY of *syn*-**9a**.

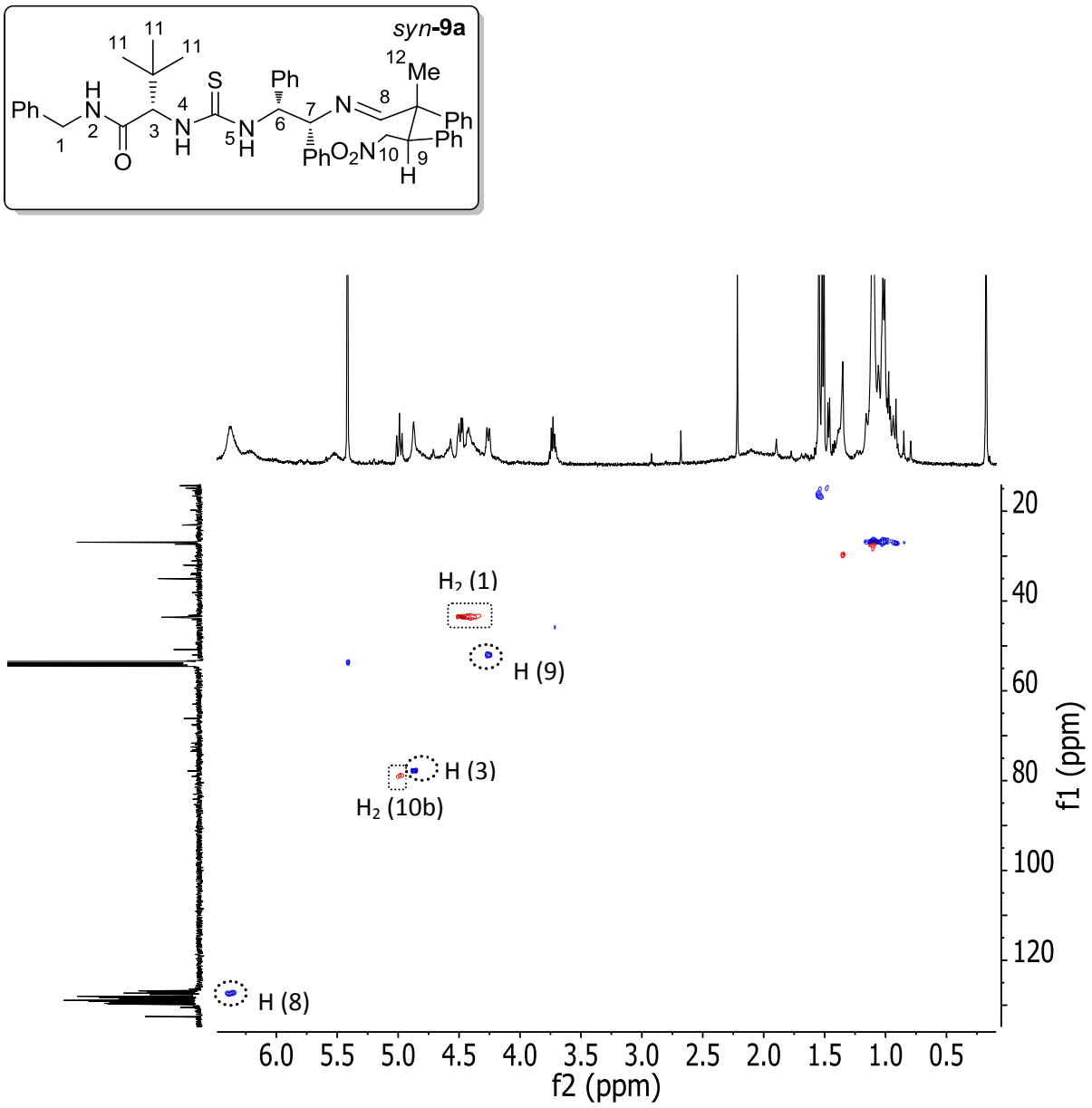

Figure S24. HSQC of *syn*-**9a**.

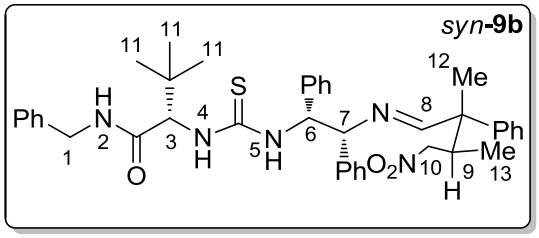

^{1}H NMR (400 MHz, $CDCl_3$) δ 0.65 (d, J = 7 Hz, 3H, CH_3), 1.04 (s, 9H, CH_3), 1.28 (s, 3H, CH_3), 3.01 (s, 1H, CH), 4.11 (t, J = 11 Hz, 1H, CH_2), 4.25-4.35 (m, 1H, CH_2), 4.35-4.45 (m, 1H, CH_2), 4.70 (br s, 1H, CH), 5.13 (br s, 1H, CH_2), 6.05 (br s, 1H, NH), 6.27 (br s, 1H, NH), 6.60 (br s, 1H, NH; 1H, CH) ppm; ^{13}C NMR (100 MHz, $CDCl_3$) δ 14.4 (CH_3), 40.1 (CH), 43.6 (CH_2), 77.5 (CH), 81.2 (CH_2), 171.4 (CH) ppm.

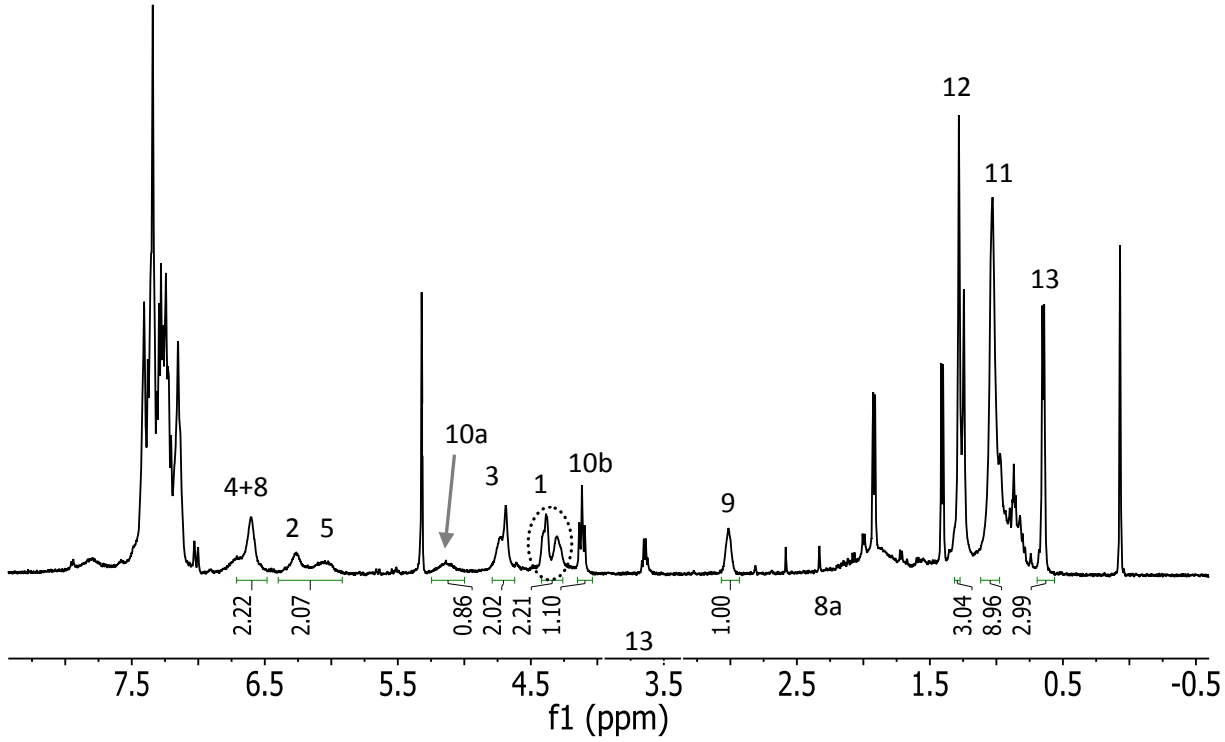

Figure S25. ^{1}H-NMR of *syn*-**9b**.

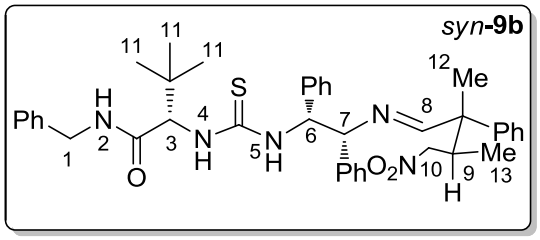

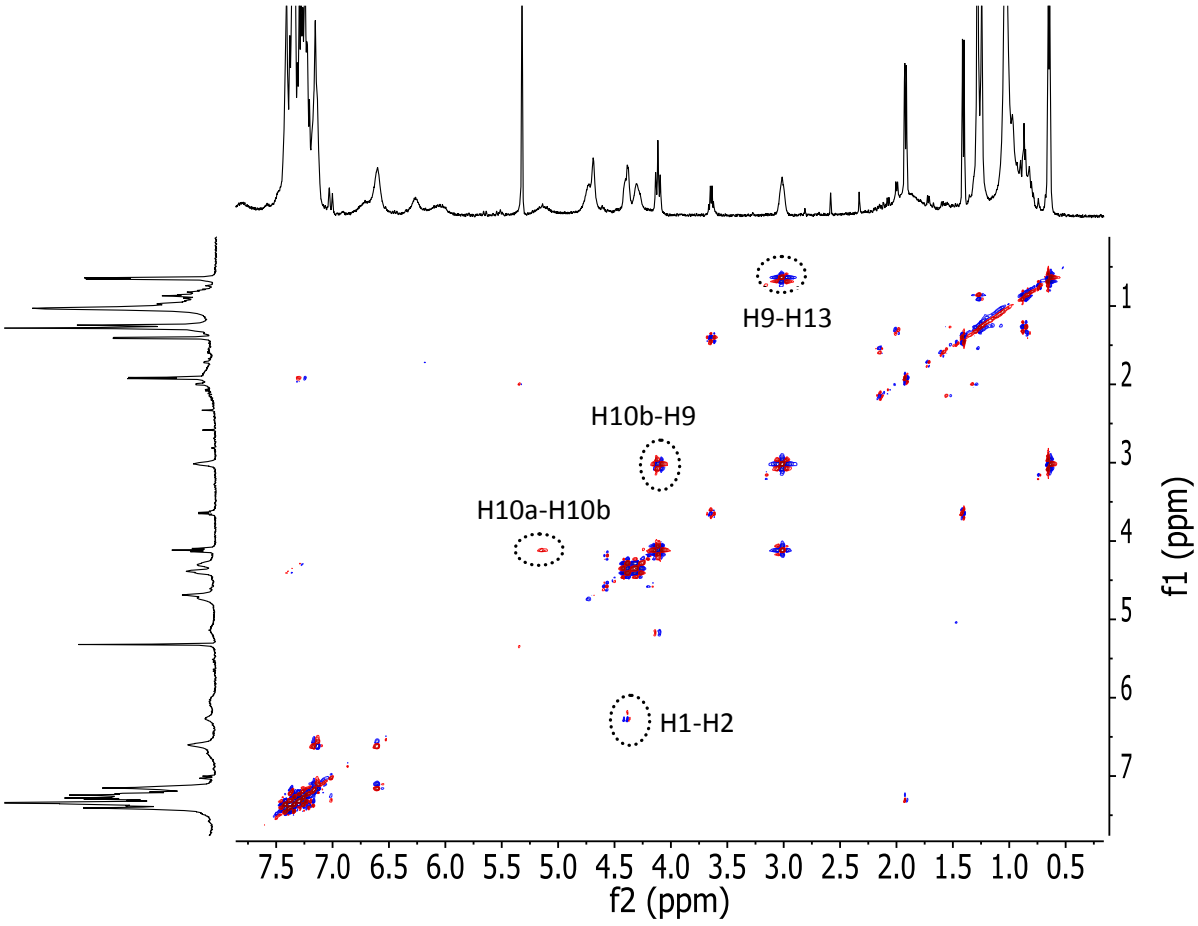

Figure S26. COSY of *syn*-**9b**.

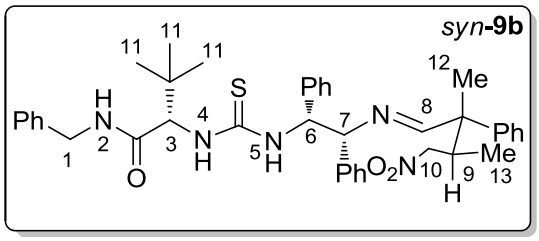

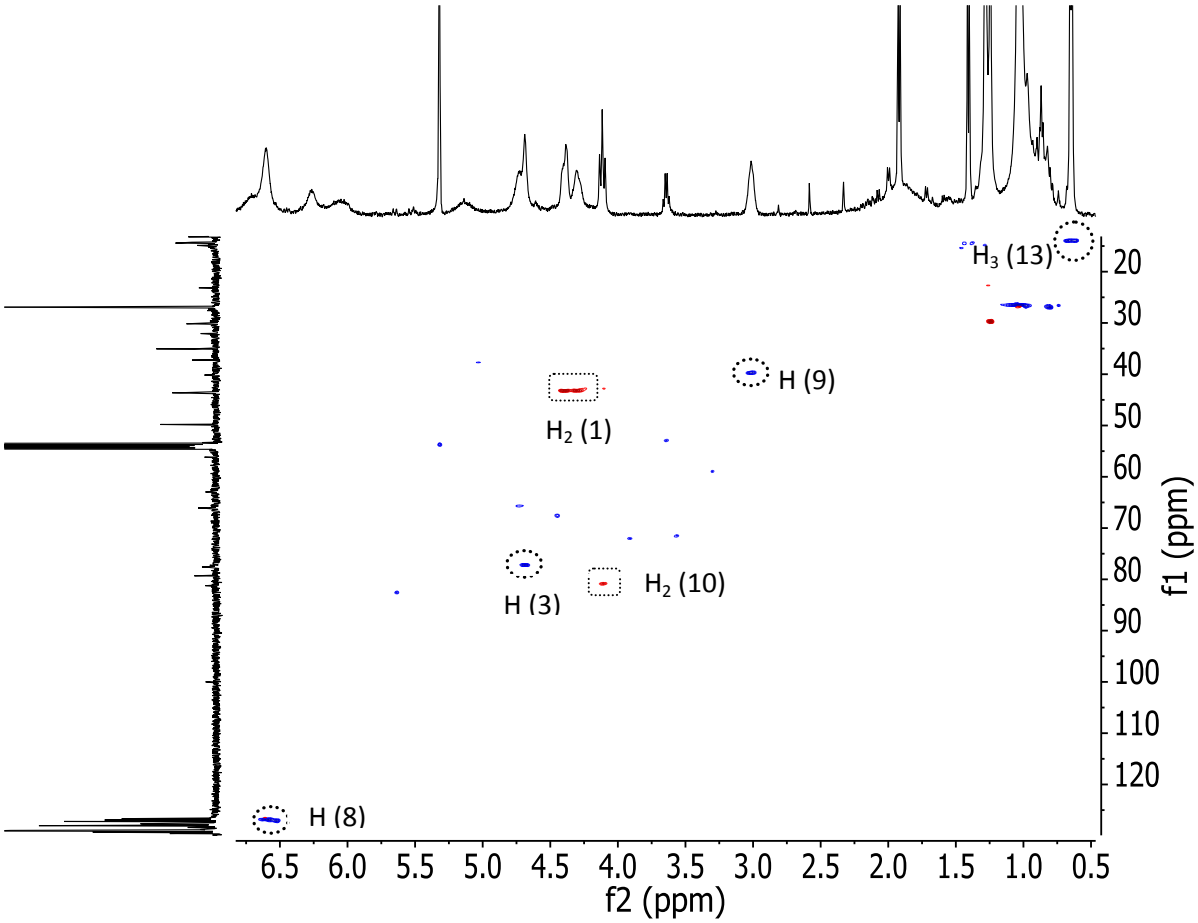

Figure S27. HSQC of *syn*-**9b**.

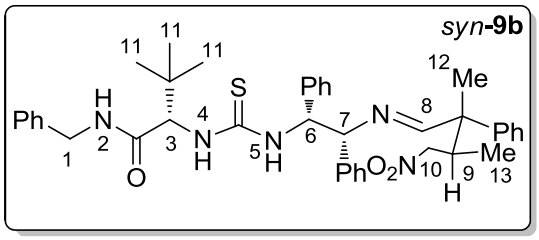

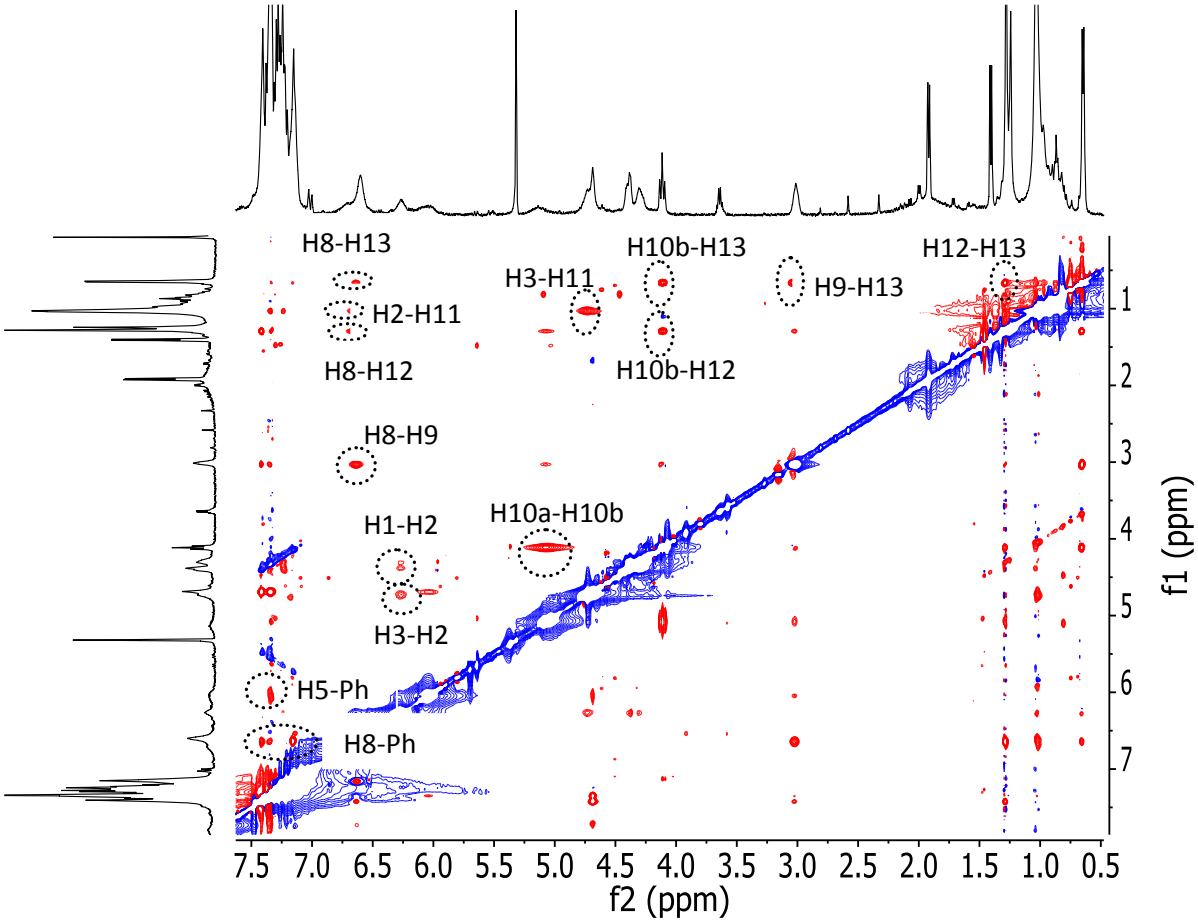

Figure S28. NOESY of *syn*-**9b**.